Available online on 15.09.2026 at http://jddtonline.info

Journal of Drug Delivery and Therapeutics

Open Access to Pharmaceutical and Medical Research

Open Access Full Text Article

Research Article

Biogenic Zinc Oxide Nanoparticles Synthesized Using *Kleinia grandiflora* Leaf Extract Suppress Triple-Negative Breast Cancer (MDA-MB-231) Through Oxidative Stress Modulation and Apoptosis

Kavithaa Krishnamoorthy[1,2*], Santhoshkumar Ravichandran[3], Senthilkumar Palanisamy[4], Sharon Rozario Solomon David [4]

[1] Centre for Cancer Research, Karpagam Academy of Higher Education (Deemed to be University), Coimbatore 641 021, Tamil Nadu, India.

[2] Department of Microbiology, Karpagam Academy of Higher Education (Deemed to be University), Coimbatore 641 021, Tamil Nadu, India.

[3] Department of Medical Biotechnology and Clinical Research, Sathyabama Institute of Science and Technology, Chennai 600 119, India

[4] Department of Biotechnology, Hindusthan College of Arts & Science, Coimbatore 641 028, Tamil Nadu, India.

Article Info:

Article History:

Received 23 June 2026
Reviewed 08 Aug 2026
Accepted 30 Aug 2026
Published 15 Sep 2026

Cite this article as:

Krishnamoorthy K, Ravichandran S, Palanisamy S, David SRS, Biogenic Zinc Oxide Nanoparticles Synthesized Using *Kleinia grandiflora* Leaf Extract Suppress Triple-Negative Breast Cancer (MDA-MB-231) Through Oxidative Stress Modulation and Apoptosis, Journal of Drug Delivery and Therapeutics. 2026; 16(9):72-83 *DOI:* https://doi.org/10.22270/jddt.v16i9.7979

For Correspondence:

Kavithaa Krishnamoorthy, Centre for Cancer Research, Karpagam Academy of Higher Education (Deemed to be University), Coimbatore 641 021, Tamil Nadu, India.

Abstract

The current investigation deals with the green synthesis of zinc oxide nanoparticles (ZnO-NPs) using aqueous leaf extract of *Kleinia grandiflora* and their physicochemical, antioxidant and anticancer properties. The synthesized ZnO-NPs were characterized using UV-Vis spectroscopy, FTIR, DLS, Zeta-potential analysis, SEM and XRD. Antioxidant property was investigated using Total phenol and flavonoid content, DPPH, FRAP assay, superoxide radical scavenger activity, Glutathione peroxidase (GPx) scavenger activity and NO scavenger assay. Anticancer activity was examined against MDA-MB-231 TNBC cell lines by MTT assay. Apoptosis was detected using acridine orange/ethidium bromide (AO/EtBr) staining. Characterization results demonstrate the formation of crystalline ZnO-NPs with characteristic physicochemical properties. The ZnO-NPs displayed concentration-dependent radical scavenging activity among all the different essays. The ZnO-NP treatment led to dose-dependent decrease in viability of MDA-MB-231 TNBC cells and the IC_{50} value was found to be around 40µg/ µmL. AO/EtBr staining confirmed the presence of morphological changes leading to apoptotic cell death. In conclusion, K. Grandiflora-mediated ZnO-NPs have good potential in the anti- TNBC therapy, in nanobiotechnology for cancer treatment, so further research is needed for the development of potential drug formulation to treat TNBC.

Keywords: *Kleinia grandiflora*, zinc oxide nanoparticles, green synthesis, triple negative breast cancer, MDA-MB-231, antioxidant activity, cytotoxicity, apoptosis, nanobiotechnology.

1. Introduction

Breast Cancer triple-negative is a sub-classification of heterogeneous malignant tumours characterized by three types of receptors; Estrogen Receptor (ER), Progesterone Receptor (PR), and Human Epidermal growth factor Receptor-2 (HER2) that all were found absent in tumour cells.[1] These three criteria are essential because of lack of the availability of hormone replacement and other targeted-therapies that rely on those receptors. Consequently, the choice of therapeutics against this sub-classification is primarily based on chemotherapy because it represents among the most deadly forms, leading a world-wide disease burden in the world, moreover, treatment outcome limitation by treatment resistance, recurrence, metastasis and toxicity has spurred development in searching new targets based on multifactor biological mechanisms such as Oxidative stress, mitochondrial dysfunction, proliferation as well as organized programmed cell death [2].

ZnO-NPs have demonstrated a promising prospect in the world of nano-medicines owing to their outstanding antimicrobial, antioxidant, optical and anticancer activities. A successful nano-medicine requires comprehensive analysis of the nature of nano-particles (NPs), including their size, morphology, crystallinity, aggregation, surface area and charge which are all highly important determinants for their bio-activity [3,4]. Nano-particles can be fabricated using number of physical and/ or chemical strategies which often involves harsh

and corrosive reactants, organic solvents, higher temperatures as well as synthetic stabilizers. However, these nano-materials can also be prepared through environmentally friendlier and milder green methods where the plant extract acts as a capping and reducing agent in which various biomolecules such as flavones, terpenoids, proteins, amino acids and carbohydrates take part in the nucleation and growth of ZnONPs [5,7]. *Kleinia grandiflora* belongs to Asteraceae family, which is rich in various Phyto-constituent and also is characterized by number of compounds with significant therapeutic potential including flavonoids, terpenes and glycosides in addition to-sitosterol and lupeol, such biochemical properties renders this plant to be a plausible bio-resource to produce nano-particles with beneficial impact against TNBC, unfortunately utilization of *K.grandiflora* in biosynthesis and application of ZnO-NPs against TNBC.[8] The previously published works on plant mediated synthesis of ZnONPs showed significant efficacy as anti-cancer agent through the generation of reactive oxygen species (ROS), induce oxidative stress, targeting mitochondria, causing genotoxicity, disrupting the cell cycle and apoptosis. [9]

Hence, here in the present study, an eco-friendly production of ZnONPs through green synthesized from *K.grandiflora* leaf extract using Phytoconstituents present in the extract which are characterized by UV-vis spectroscopy, FTIR, DLS, zetapotential, SEM and XRD; antioxidant property were estimated by DPPH, SOD, GPx, FRAP and NO assays along with total phenolics and flavonoids compounds, Moreover anticancer activity of thus synthesized ZnONPs has been examined against MDA-MB-231 TNBC cells by MTT assay followed by AO/EtBr viability assay, nuclei fragmentation imaging, and measurement of ROS in cells.[10]

2. Materials and Methods

2.1. Plant material and preparation of *Kleinia grandiflora* leaf extract

Leaves of *Kleinia grandiflora* fresh leaves were procured from local area around the botanical garden and after thoroughly washed with running tap water so as to remove the adherence of dust and foreign materials, and dried in a hot-air oven at 110-120°C for 1 week. The dried leaf was crushed to fine powder in laboratory grinder. For aqueous extraction method 10g dried powder was suspended in 100mL of distilled water (1:10, w/v) for 24-48h at 60°C. The extract cooled to room temperature and then it was filtrated by Whatman filter paper. Similarly, the extract after the sonicator can be filtered by centrifugation method at 5000rpm for 5 min and the filtered solution was used. Aqueous extract obtained was stored at 4°C till its use.

2.2. Green synthesis of ZnO nanoparticles

Green co-precipitation using *K. grandiflora* leaf extract. In detail, dried leaves 1g then crushed to powder was extract in 100ml dist. Water at room temperature for 24hr. Then, zinc acetate dihydrate 2.195 g (0.1 M) was dissolved in 100ml water and stirred at 60°C for 30 min, then mixed with 10ml extract was added dropwise. To add 1M NaOH solution until pH reached to 9-10. The mixture was stirred at 80°C for 2 hr, filtered and remained standing for overnight, centrifuged and washed by ethanol at each time. After filtering the precipitate was air-dried at 60-80°C for 24 ROS Results says "ZnO NPs synthesized using *K. grandiflora* and then kept at 4°C.

2.3. Physicochemical characterization of ZnO-NPs

The obtained ZnONPs were used for physicochemical characterization using complementary analyses that evaluate optical, surface, colloidal, morphology and crystalline characteristics. The measurements were carried out using the following methods, UV-Visible spectroscopy, Fourier-transform infrared spectroscopy (FTIR), dynamic light scattering (DLS), zeta-potential analysis, scanning electron microscopy (SEM) and X-ray diffraction (XRD).

2.3.1 UV-visible spectroscopy

The optical property of synthesized ZnONPs was measured by a UV-visible spectrophotometer. The absorption spectrum was scanning in the range of wavelengths 200-800nm for the nanoparticle suspension, to identify the optical absorption of the synthesizing material.

2.3.2 Fourier-transform infrared spectroscopy

The FTIR spectra were used to provide chemical information about the synthesized ZnONPs and to verify the interaction of biosurfactants originated from plant materials with the formed ZnONPs and the stabilisation mechanisms. FTIR was obtained in a mid-infrared region [4000-400cm-1] and the specific functional group assignment were taken from established tables of characteristic frequencies of common organic compounds or molecules present in plant species.

2.3.3. Dynamic light scattering (DLS) analysis

DLS measurement of Hydrodynamic diameter and size distribution of ZnONPs performed after dilution of nano-particle dispersion. The suspension was well dispersed before the measurement was taken and hydrodynamic diameter and particle size-distribution profile were recorded and average hydrodynamic diameter of synthesized ZnONPs and their dispersion properties were analyzed using DLS. The measurement was undertaken under standard conditions of the instrument.

2.3.4 Zeta-Potential Analysis

The surface charge of synthesized *K. Grandiflora* mediated ZnONPs, thus colloidal stability of nanoparticles in solution was determined using zeta-potential analyser. A diluted sample of ZnONPs dispersion was carefully taken and poured in electro-chemical measurement cell. The nanoparticles suspension was placed inside the instrument at specified conditions and analysed. The electrophoretic mobility of the sample nanoparticles was taken using inbuilt algorithm in the instrument and then it was used to generate zeta potential.

2.3.5. Scanning electron microscopy

Micrographs from scanning electron microscopy (SEM) were used to identify the morphological and surface features of the synthesized ZnONPs. By observation using SEM, it is possible to qualitatively identify the morphology and surface property, the size distribution and aggregation tendency of nanoparticles synthesised.

2.3.6. X-ray diffraction analysis

XRD characterization of synthesized ZnONPs to identify crystalline features and crystallographic phase was carried out. The XRD diffraction pattern was taken, and the peak positions of the observed peaks are compared and identified with respect to reference crystallographic data to study crystalline structure and crystallinity of nanostructure.

2.4. Estimation of total phenolic content

Total phenolic content (TPC): The amount of TPC of prepared ZnO-NPs was measured by an adjusted colorimetric Folin-Ciocalteu method in brief 10, 20, 30, 40 and 50 L of each sample prepared by NPs was loaded to wells, followed by add 20L Folin-Ciocalteu reagent, mixture was incubated in darkness for 3 min, then followed by add 20L NaCO solution then add 140 L H2O. The measurement of absorbance was conducted after keeping incubation in darkness for 10 min in the dark using microplate spectrophotometer on a 725nm, TPC was calculated through calculation from the calibration curve.

2.5 Estimation of total flavonoid content

The TFC was measured by aluminium chloride colorimetric method, which was slightly modified from that of other studies. Two and a half millilitres of samples was put into each well. Afterward, 2.5 mL 80% ethanol was mixed in sequence with 0.1 mL 10% aluminium nitrate and 0.1 mL potassium acetate, the mixture in the wells was swirled lightly and left in the dark at room temperature for 30-40 min. Absorbance of the samples was read at 415nm.

2.6. Antioxidant assays

2.6.1. DPPH radical-scavenging assay

Evaluation of antioxidant activity (free-radical scavenging activity) of ZnONPs was done through the DPPH assay. Various amounts of nanoparticle suspension (10, 20,30, 40, and 50mL) was then made to incubate with 195mL of DPPH solution in a 96-wellplate and was incubated for 1h in the dark at room temperature. The absorbance was measured at 540nm.

2.6.2. Ferric-reducing antioxidant power assay

FRAP activity was determined by preparing reaction mixtures composed of acetate buffer, FeCl solution and FRAP reagent. The ZnONPs of various concentrations (10, 20, 30, 40 and 50L) were added into the tube with 190L FRAP reagent and incubated at 37°C for 30min in dark. Absorbance was measured at 593nm with a microplate reader. The antioxidant capacity was expressed on the basis of the reducing power of the samples.

2.6.3. Superoxide radical-scavenging assay

The superoxide radical scavenging activity was evaluated using a reaction system using nitro blue tetrazolium (NBT), nicotinamide adenine dinucleotide (NADH) and phenazine methosulfate (PMS). The reaction mixture had 1mL NBT solution prepared in phosphate buffer (pH=7.4), 1mL of NADH solution prepared in the same buffer and varying concentrations of the ZnO-NP preparation. The reaction was started after adding 100µL of PMS solution and then incubated at room temperature for about 5min. The absorbance was measured at 560nm. Ascorbic acid was used as a reference antioxidant and the percentage inhibition was calculated as

2.6.4. Glutathione peroxidase activity

GPx activity was measured by adding potassium phosphate buffer (pH 7.0), sodium aside, reduced glutathione (GSH), hydrogen peroxide, distilled water and different amount of ZnONP preparation into the solution and incubated at 37°C for 3 minutes, then 10% tri-chloroacetic acid was added to stop the reaction, after 3000 rpm centrifugation at 30°C for 5 minutes, 50µL supernatant was added 100µL 0.3M KHPO4 and 50µL 0.04% DTNB, then A 412 nm was collected after 3 minutes.

2.6.5. Nitric oxide-scavenging assay

The nitric oxide-scavenging activity was measured by the Griess reaction. After incubation for 150 min at 37°C, 100L of recently prepared Griess reagent was added to the reaction mixture. The Griess reagent was prepared by adding the equal volume of the solution, consist of 0.1% (w/v) naphthyl ethylenediamine dihydrochloride, and 1% (w/v) sulphanilamide dissolved in phosphoric acid. Then the solution was shaken, allowed to stand for 5 min, and the absorbance was taken at 540nm wavelength.

2.7. In-vitro anticancer activity

2.7.1. Cell culture and treatment

MDA-MB-231 TNBC cells were acquired from NCCS, Pune, India and were cultured in DMEM supplemented with 10% fetal bovine serum (FBS), 2% essential amino acid, 2% penicillin-streptomycin solution at 37°C under 5% CO. Cells were seeded in 96-well plates for cell cytotoxicity test and 6-well plates with coverslip for fluorescent staining. Treated group was classified into three- groups which are untreated control, ZnONPs treated cell, *K. Grandiflora* leaves extract treated cell and K.

2.7.2. MTT cytotoxicity assay

3.2 MTT Assay Cytotoxicity of ZnO-NPs synthesized has been carried out using MTT assay (Ohtsu et al., 1998). Different Concentrations of ZnO-NPs was added to MDA-MB-231cells then were incubated with 50L MT reagent (3µg/mL PBS) at 37°C for 3h. The formazan crystals produced was then dissolve with isopropanol-Acidification. Absorbance was determined at 650 nm with a micro- plate reader. Percentage cell-viability was expressed relative to the untreated control cells. IC_{50}

value was determined from a concentration response curve.

2.7.3. AO/EtBr fluorescence staining

Cellular changes related to apoptosis were evaluated by AO/EtBr stain. Cells were stained with 10 L AO/EtBr working solution, incubated for 5 min at room temperature and observed under fluorescence microscope at 400 magnifications. Live cells were observed as brightly green fluorescing and apoptotic cells were seen as differently fluorescent, with condensed nuclei or nuclear fragmentation.

2.7.4 DAPI nuclear staining

Nuclear morphology changes in cells after treatment of ZnO-NPs After treatment of ZnO-NPs, apoptosis caused the change of nuclear morphology, cells were collected from sterile cover slip placed on sterile cover slip then washed with PBS, fixed and stained with DAPI incaverningroom dark. Cells were viewed with fluorescence microscopy, mountedonslidingand evaluated by fluorescence microscopic observer. Nuclei were condensed or fragmentation noted was considered as related with the early stages of apoptosis.

2.7.5 Intracellular reactive oxygen species determination

Determination of intracellular ROS accumulation after ZnONPs treatment. Intracellular ROS production in cells post-treatment with ZnONPs was assessed using a dichlorofluorescein-based fluorescence assay. Briefly, MDA-MB-231 cells were grown and exposed to the designated concentration of ZnO-NPs. Cells were then rinsed with PBS followed by incubation with the ROS-sensitive fluorescent probe 2,7-dichlorodihydro-fluorescein diacetate (DCFH-DA) under light protection. After internalized by cells, DCFH-DA is hydrolysed to nonfluorescent DCFH by esterase and oxidized to fluorescent DCF by ROS within the cells. Cells were washed with PBS and fluorescent intensities detected through a fluorescence microplate reader or flow cytometer depending on instrument available. Increased intracellular DCF fluorescence relative to negative control indicated a higher level of accumulation of cellular ROS.

3. Results

3.1. UV-visible spectroscopic analysis

Optical Characterizations Ultraviolet – Visible (UV-Vis) spectroscopy (0 - 600 nm) was performed on the obtained ZnO-NPs and the UV-Vis absorption spectrum is illustrated in **Figure 1.** The spectrum shows a large absorption at ~245nm and a decreasing intensity over higher wavelengths towards the visible region. This intense UV absorption is a definite indicator of the formation of nano-sized ZnO. There is no conspicuous band present in the visible region indicating no significant absorption owing to strongly coloured secondary phases in the resulting ZnO-NPs.

Based on the obtained UV-Vis absorption spectrum and correlating with the FTIR and XRD data obtained for the sample, we were convinced that ZnO-NPs were successfully prepared.

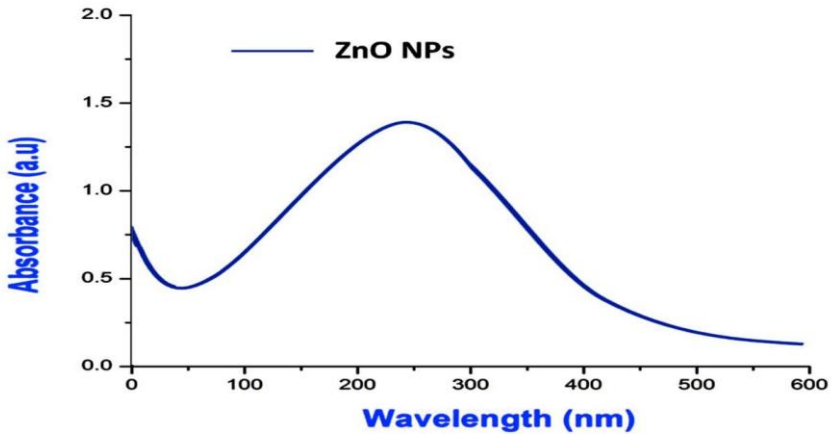

Figure 1: UV- Visible absorption spectrum of zinc oxide nanoparticle

(UV–Visible absorption spectrum (a)

3.2 FTIR analysis

To know the functional groups of the synthesized *K. Grandiflora* - mediated ZnONPs, FTIR spectroscopy was carried out for the understanding of their potential contribution to the formation of NPs. A spectrum with some peaks in the region between 600 and 4000 cm^{-1} were obtained. Peak at 3319cm^{-1} belongs to O-H stretching whereas the peaks at 2944 and 2830 cm represents to C-H (aliphatic) stretching (Figure 2). Peaks ranging between 1715–1649 cm represented the carbonyl group or C=C group and peaks at 1466, 1403, 1320, 1240, 1145and 1068cm represent the containing of oxygen (Figure 2). Therefore, it could be suggested that *K. Grandiflora* phytochemical was participate in surface capping and formation of ZnONPs. **(Fig. 2)**

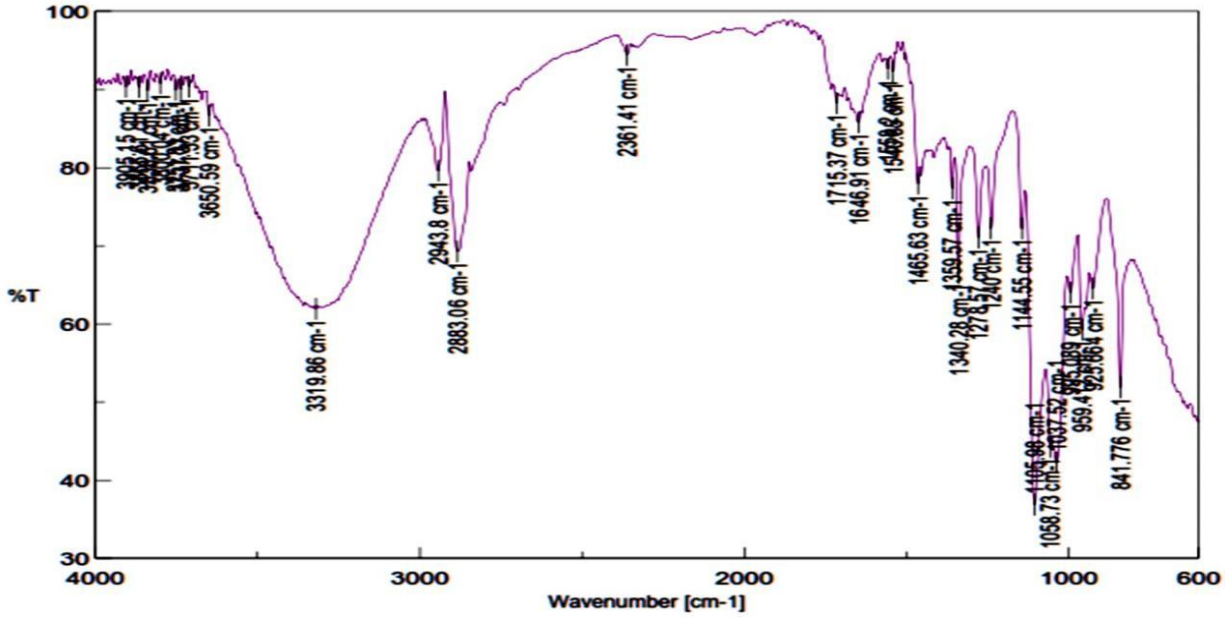

Figure 2: FT-IR spectrum of zinc oxide nanoparticle

FTIR spectrum of *Kleinia grandiflora*-mediated ZnONPs showing the characteristic vibrational bands associated with ZnO and phytochemical-derived

3.4. Dynamic light scattering

DLS was carried out to determine the hydrodynamic size distribution of the synthesized ZnONPs in aqueous suspension. An intensity-based size-distribution profile resulted, which had one major sharp peak with a size of approximately 150nm **(Fig. 3).** The measured hydrodynamic diameter suggested that the nanoparticles were primarily within the nanoscale range. The DLS measurement resulted in a major hydrodynamic diameter near 150 nm, which means that the particles size is about nanoscale of particles, surrounded by hydration and potential surface attached biomolecules. The sharp distribution seen in the intensity profile indicates primarily nanoparticle size, although a degree of aggregation cannot be ruled out.

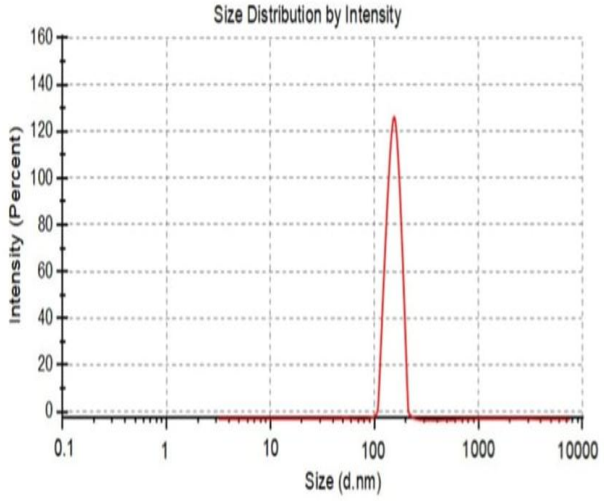

Figure 3: Dynamic light scattering profile of zinc oxide nanoparticle

Dynamic Light scattering size-distribution profile of *Kleinia grandiflora* mediated ZnONPs revealing mainly one population of hydrodynamic particle sizes in water suspension.

3.5. Zeta-potential analysis

The surface charge properties of the as synthesized ZnONPs were assessed through zeta-potential measurements. Fig. 4 shows a narrow band (primary distribution with a population maximum of negatively charged SNPs in the region between approximately 10 and 20 mV) with a small second population at positively charged zeta-potential. The primarily negative zeta potential arises due to adsorption of the phytochemical negatively-charged molecules onto the ZnONPs via their hydroxyl, carboxylate or phenolic functionalities and other groups containing oxygen atoms of *K. Grandiflora* extract and thus gives supporting information on interaction of biomolecules extracted from plant with nano Particles as reported earlier.

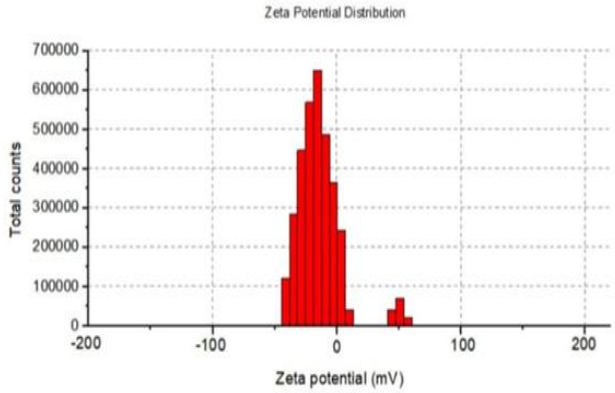

Figure 4: Zeta potentials of zinc oxide nanoparticle

Zeta-potential distribution of *Kleinia grandiflora* - mediated ZnONPs. Here, the surface-charge distribution of the nanoparticle suspension is represented.

3.6. SEM analysis

SEM characterization showed that the as-prepared ZnONPs were of irregular morphology to quasi-spherical with poor monodispersed and partial aggregation, appearing as numerous nanoscale dots and large islands **(Fig. 5).** Aggregation of nanoparticles likely resulted from the inherent tendency due to the large surface area-to-volume ratio and possible agglomeration of nanoparticles during dehydration and sample treatment prior to observation by SEM. The SEM results demonstrate, however, nanoscale formation of ZnO material although complementary information from DLS for nanoparticle behaviour in the aqueous dispersion are required.

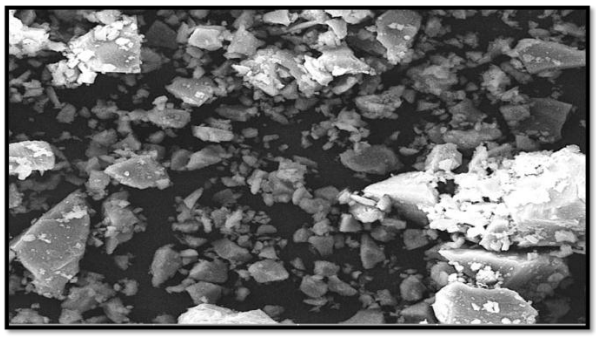

Figure 5: Scanning electron micrograph of zinc oxide nanoparticle

SEM image of *Kleinia grandiflora*-derived ZnONPs exhibiting shape, size and agglomeration patterns.

3.7. X-ray diffraction analysis

The XRD pattern of ZnONPs was shown in the **Fig. 6**. Three prominent diffraction peaks were obtained around 31.7, 34.4, 36.2, 47.5, 56.6 and 62.9 are representing the characteristic crystal reflections of ZnO which can indexed to the (100), (002), (101), (102), (110), and (103) planes respectively in order to confirm that the *K. Grandiflora* plant extract supported ZnONPs are in hexagonal wurtzite crystal phase formation. There were additional mild peaks at larger values of 2θ possibly resulting from the interference of other high-angle crystallographic plane diffraction signals.

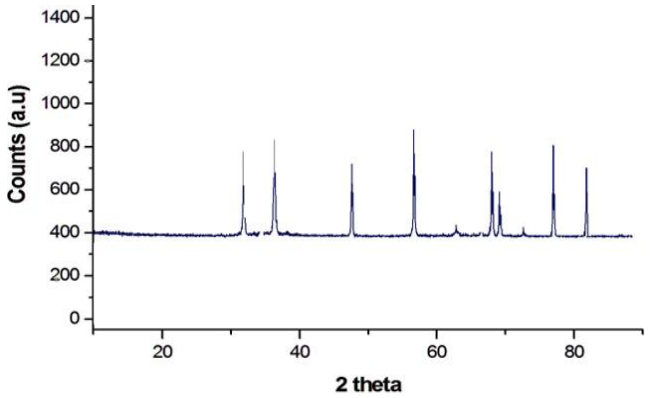

Figure 6: XRD pattern of zinc oxide

XRD pattern of ZnONPs formed by *Kleinia grandiflora*-mediated formation where characteristic reflection peaks associated with pure ZnO crystalline phase.

3.8. Total phenolic content

The Folin-Ciocalteu assay was used to assess the phenolic linked properties of the synthesized ZnONPs. The observed absorbance was dependent on the concentration of the nanoparticle preparation being tested, an increasing absorbance was measured from 0-5µg/mL **(Fig.7).** An increasing absorbance from approx. 0.30 at 0µg/mL to 0.64 at 5µg/mL. The increase in absorbance demonstrates the presence of compounds that react with the Folin-Ciocalteu reagent that could be linked to the nanoparticle preparation and may have been derived from the phenolic compounds present within the *K. Grandiflora* extract, helping to form and functionalize the nanoparticles.

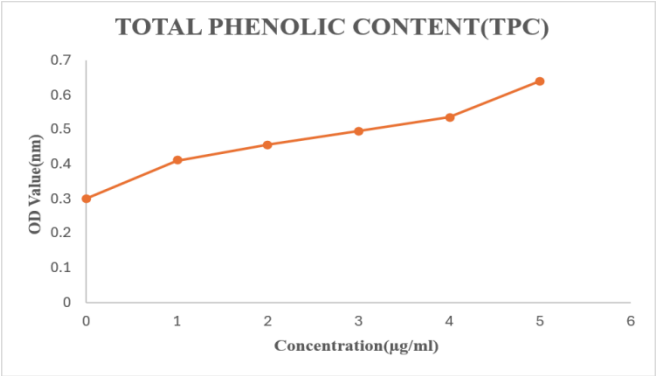

Figure 8: Total phenolic content of zinc oxide nanoparticles

TPC of ZnONPs synthesized using *Kleinia grandiflora* at various concentrations. Values shown are measured OD value at 725nm.

3.9. Total flavonoid content

Also, there is a significant and concentration dependent increase on the total flavonoid-associated response in the extract ZnONP composite **(Fig. 8).** The observed change of the absorbance in time gradually increased from 1.71 in 0µg/mL to 1.89 in 5µg/mL. Therefore, presence of aluminium-chloride-reactive flavonoid-associated components which might have remain bound to the surface of the ZnONPs even after green synthesis process may act as bio-available agents in the plant extract and could participate in the biological effects observed in the extract ZnONP composite.

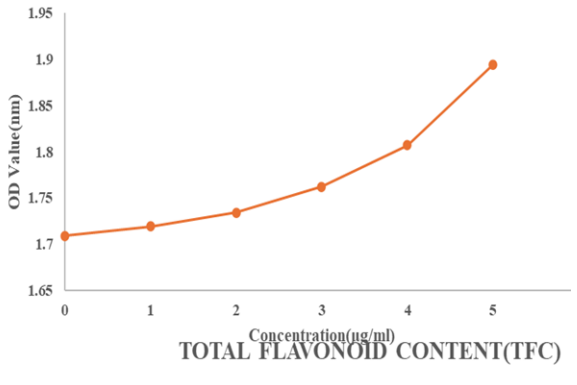

Fig 9: Total flavonoid content of zinc oxide nanoparticles

Total flavonoid content (TFC) of *Kleinia grandiflora*-mediated ZnONPs at different doses. Values indicate the measured response by optical density after using blank at the 415nm.

3.10. DPPH radical-scavenging activity

Synthesized ZnONPs showed concentration-dependent DPPH free radical scavenging capability for the test concentration of 10-50µg/mL **(Fig. 9).** The scavenging capability showed a proportional increase with increasing concentration of the synthesized ZnONPs, and the maximum scavenging capacity maintained from 82-85% concentration with 50µg/mL of synthesized nanoparticle. It is observable there is lower percent scavenging compared to ascorbic acid for all tested concentrations in this study. A significant difference was observed between the test and standard at each tested concentration, $p<0.01$ was obtained at all tested concentrations in this study. The free radical scavenging activity increased in proportion with the test concentration it is assumed many of the phytochemical bind green synthesize ZnONP worked as free radical scavengers.

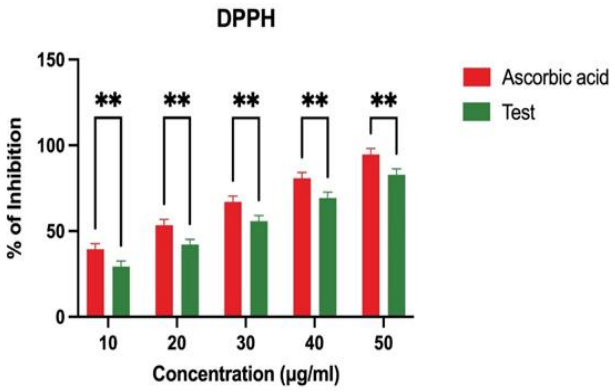

Figure 9: DPPH antioxidant assay

2,2-Diphenyl-1-picrylhydrazine (DPPH) radical scavenging capacity of *Kleinia grandiflora* -mediated ZnONPs in comparison with different concentrations of Ascorbic acid. Each bar represents mean SD.

3.11. Ferric-reducing antioxidant power

The reducing activity was expressed in percentage compared to ascorbic acid that yielded more activity along the increasing concentrations. **(Figure 10).** FRAP analysis indicated a concentration-dependent enhancement of the ZnONPs reducing activity (Fig. 10). Its activity grew from circa 24% to 70% when passing from 10µg/mL to 50µg/mL. In the reference group, the activity was greater through all concentrations. There were no differences that would have shown significant results at 10-30µg/mL, but when applying 40µg/mL and 50µg/mL, we got statistically significant differences, so we can report that the reducing power of ZnONPs grew with increasing concentration but still the results were lower when using higher concentrations when compared with the ones used as antioxidant references.

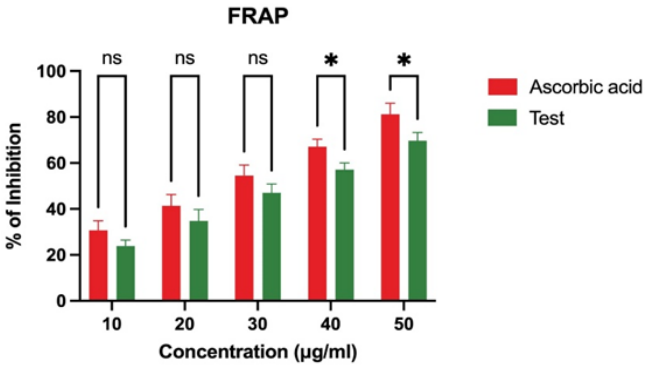

Figure 10: FRAP antioxidant assay

Ferric-reducing antioxidant capacity (FRAP) values between *Kleinia grandiflora*-mediated ZnONPs and ascorbic acid in a range of concentrations. Values represent mean S.D.$p < 0.05$; ns, non-significant.

3.12. Superoxide radical-scavenging activity

Superoxide radicals. The ZnONPs demonstrated good activity across the range of concentrations, **(Fig. 11).** The scavenging response increased from about 30% at 10µg/ml to 65% at 50µg/ml. The ZnO-NP preparation demonstrated a significantly higher activity than that of ascorbic acid at every concentration of test (the difference shown on the graph is $P<0.01$ at 10µg/ml, and $P<0.001$ for concentrations ranging from 20µg/ml to 50µg/ml). This indicates the nanoparticle preparation has significant potential to scavenge these reactions which relate to oxidative processes dependent on superoxide.

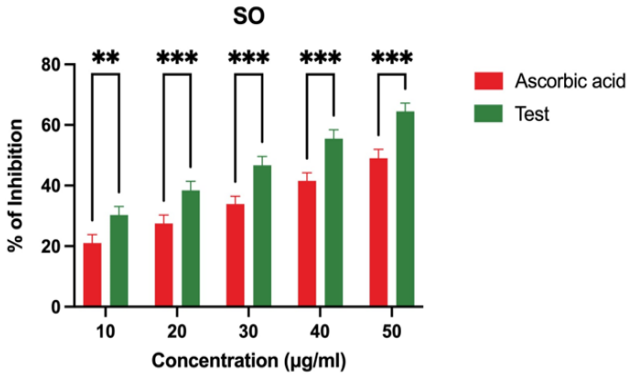

Figure 11: SO, antioxidant assay

Superoxide radical-scavenging activity of *Kleinia grandiflora*-mediated ZnO-NPs compared with ascorbic acid at different concentrations. Data are presented as mean ± SD. *$p < 0.01$; **$p < 0.001$.

3.13. Glutathione peroxidase-associated activity

Fig 12 The GPx assay show that the calculated enzyme-associated antioxidant activity of the ZnO-NP preparation is increasing in a concentration-dependent manner ranging from approximately 15% at 5µg/ml to approximately 30% at 100µg/ml. Standard provided a larger activity than the sample at all tested concentrations; however, it indicates concentration-dependent antioxidant response in the system.

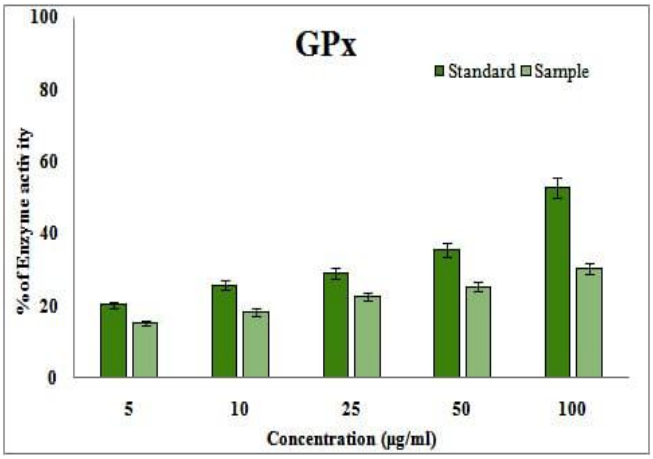

Figure 12: Glutathione peroxidase-associated activity

Effect of *Kleinia grandiflora* treated ZnONPs on Glutathione peroxidase (GPx)-like activity as compared with control in varying concentrations. Values were expressed as mean SD.

3.14. Nitric oxide-scavenging activity

The nitric oxide-scavenging activity, shown in **Fig. 13**, was concentration-dependent; its activity, after administration of ZnONP, was seen to rise from nearly 32% in 10µg/mL to nearly 71% in 50µg/mL. Interestingly, the developed ZnONP was noticed to be more active in scavenging nitric oxide radicals than was ascorbic acid in all of the trials and a highly statistically significant difference can be found, with p values from $p < 0.05$ up to $p < 0.01$. As these results have pointed out, the obtained ZnONPs have shown significant amounts of nitric oxide-scavenging activity too that strengthen DPPH, FRAP, superoxide, GPx test results in determining that these particles may possess significant amounts of antioxidant property.

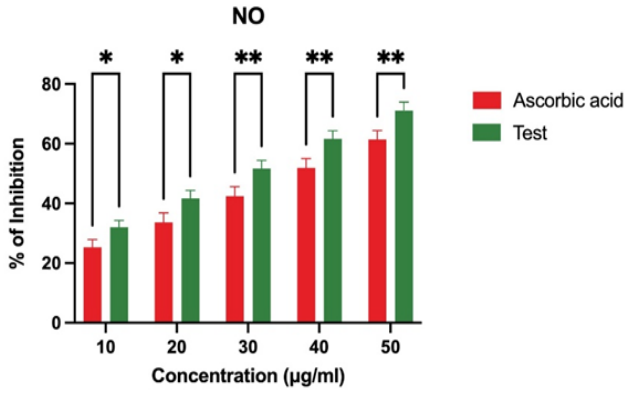

Figure 13: NO2 antioxidant assay

Nitric oxide (NO)-scavenging activity of *Kleinia grandiflora*-mediated ZnONPs compared with ascorbic acid at different concentrations. Data are presented as mean ± SD. Statistical significance is indicated by asterisks.

3.15. Cytotoxicity of ZnO-NPs against MDA-MB-231 cells

Fig. 14 represents the comparative cytotoxic viability assessment conducted against the triple-negative breast cancer cell line (MDA-MB-231 cells). ZnO-NPs effectively cause a dose-dependent decrease in the cell viability wherein 95%, 62%, 54%, 35% and 30% of cells are viable in the presence of 5, 10, 25, 50 and 100 g/mL, respectively whereas that of doxorubicin were found to be 58%, 32%, 22%, 20% and 18%, respectively, exhibiting better efficacy of doxorubicin as an anticancer agent against theMDA-MB-231 TNBC cells. ZnO-NPs demonstrated a dose-dependent cytotoxicity clearly whereas were slightly less effective. IC_{50}values based on the calculated dose-response equation derived from non-linear regression of each set (Fig. 14) against the dose indicates the cytotoxicity as between 25 and 50µg/mL.

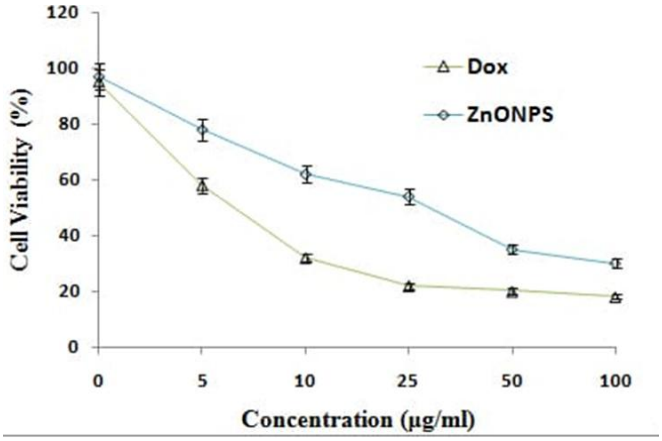

Figure 14: Zinc oxide nanoparticle compared with standard doxorubicin

Cytotoxicity of ZnONPs and doxorubicin dependent on its concentration towards MDA-MB-231 triple-negative breast cancer cells.

3.16. AO/EtBr staining

Morphological changes in MDA-MB-231 cells on ZnONPs treatment was analysed using AO/EtBr staining showing concentration dependent cellular damages **(Fig. 15).** Normal/control cells displayed a strong green fluorescence and normal cell morphology that are viable. In contrast, ZnO-NP-treated cells display increased level of yellow/orange and red fluorescence with cellular deformation indicating compromised integrity and apoptosis. Increased conversion from green to yellow/orange and red fluorescence was observed at higher concentrations of ZnONP leading to elevated numbers of cells undergoing apoptosis/late stage of death.

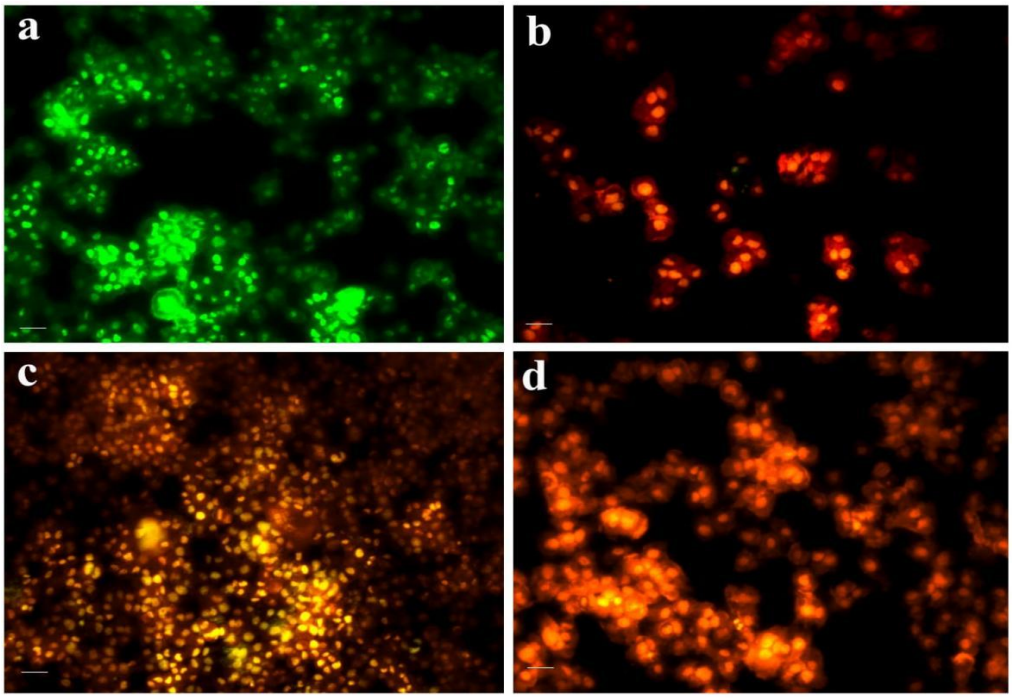

Figure 15: Differentiation of live and apoptotic cells by AO/EtBr staining

MDA-MB-231 cell morphology and AO/EtBr fluorescent signals after treatment with *Kleinia grandiflora* - mediated ZnONPs at increasing concentrations, demonstrating dose-dependent cellular fluorescence alteration with apoptosis.

3.17. DAPI nuclear staining

Nuclear morphologic changes in MDA-MB-231 cells were examined using DAPI staining after treating with *K. Grandiflora*-mediated ZnO-NPs **(Fig 16).** In control cells, normal and homogeneous nuclei were observed (Fig. 16a). Concentration-dependent change of nuclear morphology was observed in treated cells (Fig. 16b-d). It revealed cell nuclei fragmentation, condensed nuclei and irregular shape of nuclear. Condensed nuclei and fragmented structure of nucleus in treatment were correlated with apoptosis. Increase of abnormality in nucleus was consistent with AO/EtBr staining result that cell morphology changes with different concentration, indicating the characteristic of apoptotic cells.

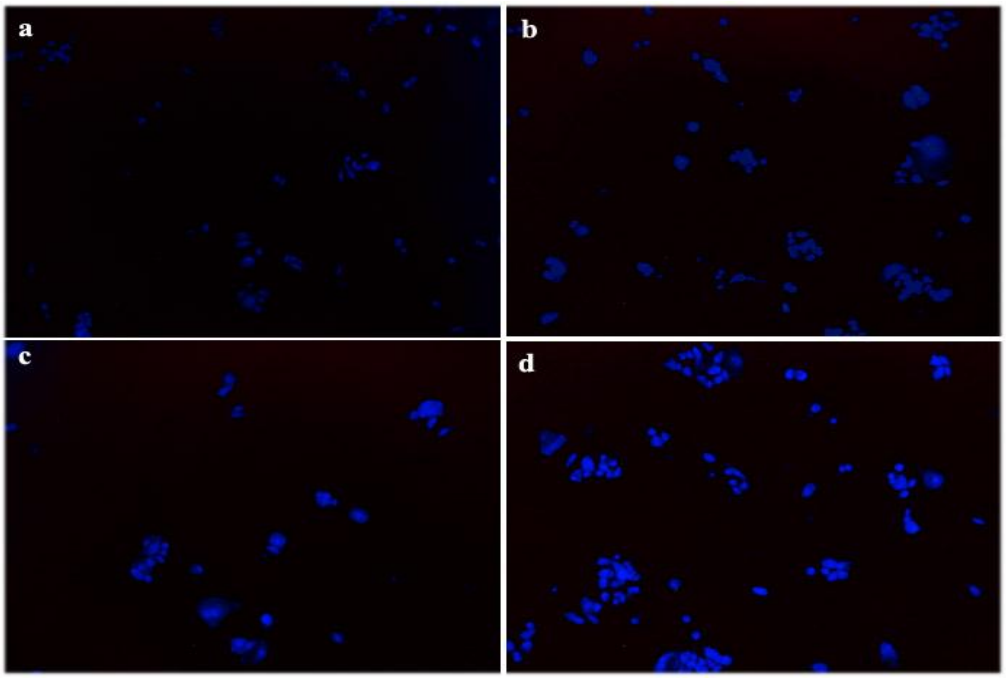

Figure 16. DAPI fluorescence staining

Figure 16. Effects of *K. Grandiflora*-derived ZnONPs treatment on DAPI fluorescent staining ofMDA-MB-231 cells. (a)untreated; (b-d) cells treated with ZnONP-producing from extract, revealing increasing changes of nuclear morphology, including condensation and fragmentation.

3.18. Intracellular ROS Generation

ROS production within cells the amounts of intracellular ROS production were monitored upon treatment of ZnO NPs synthesized using *K. Grandiflora* leaf on MDA-MB-231 cells **(Fig. 17).** Minimal green colour was present in cells treated as a control. Cells treated with increase concentrations of K. Grandiflora mediated ZnO NPs showed increasingly distributed green coloration (Fig. 17a-d). Highest treatment with highest concentration of ZnONPs led to brightly, green coloured dispersed in cells implying accumulation of intracellular ROS and disruption of homeostasis for ROS. Rise in ROS production was followed with decline in cell viability and morphological changes in cell. The accumulation of intracellular ROS possibly resulted in damage to the biological macromolecules such as lipids, proteins, DNA, RNA and other.

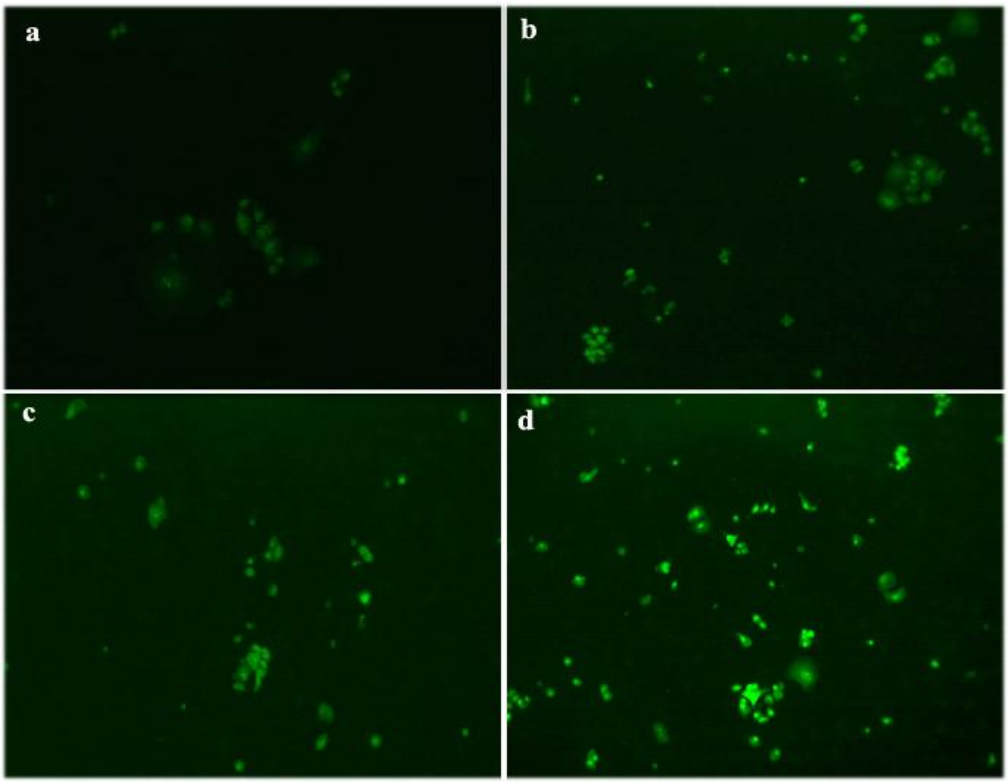

Figure 17. Intracellular ROS fluorescence

Fig 17. Intracellular ROS level after treatment with *K. Grandiflora* ZnONPs. (a) untreated control, (b,c,d) cells treated with ZnONPs revealing increasing levels of green fluorescence representing improved generation of ROS.

4. The Discussion

In this study, the green synthesis of ZnO-NPs utilizing *K. Grandiflora* leaf extract was achieved and the physical, chemical and biological characteristics were completely evaluated. The absorption maxima at nearly 245 nm and FTIR and XRD results confirm the formation of ZnO-NPs. The bands that are related to hydroxyl (O-H), aliphatic functional group (-CH), carbonyl/C=C, and other oxygen-containing functional group imply the involvement of plant phytochemicals for biosynthesis and capping of nanoparticles.[11]

The result from DLS shows particle size was about 150nm hydrodynamic diameter, SEM image shows irregular to quasi-spherical morphology. The size of the dispersed particle may be influenced by partial aggregated structure and aqueous nature. The mostly negative zeta potential might be caused by adsorption of negatively charged functional parts of phytochemical molecules onto nanoparticle surface. [12,13] The result from XRD revealed crystalline structure with hexagonal wurtzite framework of ZnO-NPs. The appearance of the reactions related with phenolic and flavonoid group show the coexistence of phytochemical. The result of colorimetric assays for antioxidant activities proved the existence of reacting groups but not identify or quantify precisely what the individual phytochemical molecules. [14,15]

The ZnONPs showed dose-dependent effect in all DPPH, FRAP, Superoxide Radical, GPx, and NO activity. Differences in DPPH, FRAP, superoxide, GPx and NO activity were due to variations in radical species and reaction mechanism. In addition, the ZnONPs displayed dose-dependent cell viability inhibitory activity toward MDA-MB-231 cell. [16] Interaction between ZnO-NPs and cell, zinc ions from nanoparticles' disintegration in cells and oxidative stress caused by nanoparticle, phytochemical adsorbed in ZnO-NPs surface can all result in the antiproliferation.

AO/EtBr staining showed the changes in morphology and fluorescence in dose-dependent manner, while DAPI staining revealed the characteristics of condensed and fragmented nuclei, which indirectly demonstrate apoptosis induced damage on cell and nucleus but the explicit cell death pathway is not concluded. [17,18] Furthermore, the data on elevated ROS level supports the existence of oxidative stress which leads to cell death. Proposed cascade should be ZnONPs exposure, accumulation of intracellular ROS, oxidative stress leading to cell and nucleus damage and apoptosis, ultimately cell death with reduced cell viability. However, correlation is not equivalence, thus Annexin V/PI analysis, mitochondrial membrane potential, activity assay of caspase and related genes should be done to verify cell apoptosis pathway. [19-21]

5. Conclusion

In the current research work, the green synthesis of ZnONPs using *K. Grandiflora* leaf extract was successfully prepared along with it physiochemical and biological characteristics were studied. It was revealed in UV-Vis and FTIR analysis the presence of nano-structures and presence of phytochemical associated functional groups in the stabilization of surface of ZnONPs. The determined hydrodynamic size was about 150nm by DLS and it was also stated that the generated ZnO-NPs had majority negative surface charge on it in zeta-potential study. From SEM it was noticed that the shape is partially aggregation, and the morphologies vary from irregularity to quasi-spherical while it is crystalline hexagonal wurtzite as seen from XRD. The prepared ZnONPs had a dose-responsive free radical scavenging activity towards DPPH, FRAP, super-oxide, GPx, nitric oxide potentially related to the phenolic and flavonoid component of *K. Grandiflora*. The synthesized ZnO-NPs were found to be dose-responsive cytotoxic against MDA-MB-231 TNBC cells and also revealed presence of apoptotic cell and nuclear changes through the staining using AO/EtBr and DAPI, and accumulation of intracellular ROS showed that oxidative stress could be one of the reasons for such cytotoxic response of the synthesized nanomaterial, which was also found from AO/EtBr and DAPI staining.

Overall*, K. Grandiflora* synthesized ZnO-NPs may be a potentially useful green-synthesized anti-cancer and free radical scavenging agent for TNBC and in future researches, it may work in selective range of normal-cell as well which can be seen through Annexin V/PI analysis and cell-cycle progression, mitochondrial membrane potential, caspase activity, apoptosis relevant gene and protein expression studies, as well as in-vivo study has to be done for actual clinical application.

Acknowledgement: The authors sincerely acknowledge NexCell Biotech Lab for providing the necessary facilities and technical support to carry out the experimental work of this study.

Consent to Participate: Not Applicable

Consent for Publication: Not Applicable

Declaration of Conflicting Interests: The authors declare that there are no conflicts of interest associated with this work.

Ethical Approval: Not Applicable

References

1. Bianchini, G., Balko, J. M., Mayer, I. A., Sanders, M. E., & Gianni, L. Triple-negative breast cancer: Challenges and opportunities of a heterogeneous disease. *Nature Reviews Clinical Oncology,* 2016;*13*:674–690. https://doi.org/10.1038/nrclinonc.2016.66

2. Dent, R., Hanna, W. M., Trudeau, M., Rawlinson, E., Sun, P., & Narod, S. A. Pattern of metastatic spread in triple-negative breast cancer. *Breast Cancer Research and Treatment,* 2009;*115*:423–428. https://doi.org/10.1007/s10549-008-0086-2

3. Bianchini, G., Balko, J. M., Mayer, I. A., Sanders, M. E., & Gianni, L. *Nature Reviews Clinical Oncology,* 2016;*13*:674–690.

4. Mitchell, M. J., Billingsley, M. M., Haley, R. M., Wechsler, M. E., Peppas, N. A., & Langer, R. Engineering precision nanoparticles for drug delivery. *Nature Reviews Drug Discovery,* 2021;*20*:101–124. https://doi.org/10.1038/s41573-020-0090-8

5. Bayda, S., Adeel, M., Tuccinardi, T., Cordani, M., & Rizzolio, F. The history of nanoscience and nanotechnology: From chemical–physical applications to nanomedicine. *Molecules,* 2020;*25*(1):112. https://doi.org/10.3390/molecules25010112

6. Vera, J., Herrera, W., Hermosilla, E., Díaz, M., Parada, J., Seabra, A. B., Tortella, G., Pesenti, H., Ciudad, G., & Rubilar, O. Antioxidant Activity As an Index for the Efficacy of the Plant Extract-Based Synthesis of Zinc Oxide Nanoparticles. Antioxidants, 2023;12(4):784. https://doi.org/10.3390/antiox12040784

7. Sivasankarapillai, V. S., Krishnamoorthy, N., Eldesoky, G. E., Wabaidur, S. M., Islam, M. A., Dhanusuraman, R., Ponnusamy, V. K., 2022.

8. Al-darwesh, M. Y., Ibrahim, S. S., & Mohammed, M. A. A review on plant extract mediated green synthesis of zinc oxide nanoparticles and their biomedical applications. *Results in Chemistry,* 2024;*7*:101368.

9. Sivasankarapillai, V. S., et al. One-pot green synthesis of ZnO nanoparticles using *Scoparia dulcis* plant extract for antimicrobial and antioxidant activities. *Applied Nanoscience,* 2022;*12*:2731–2743.

10. Pouresmaeil, V., Haghighi, S., Raeisalsadati, A. S., Neamati, A., & Homayouni-Tabrizi, M. The anti-breast cancer effects of green-synthesized zinc oxide nanoparticles using carob extracts. *Anti-Cancer Agents in Medicinal Chemistry,* 2021;*21*(3):316–326. https://doi.org/10.2174/1871520620666200721132522

11. Mongy, Y., & Shalaby, T. *Scientific Reports,* 2024;*14*:13470. https://doi.org/10.1038/s41598-024-63258-7

12. Tegegne, B. A., Begashaw, T., Belay, W. Y., et al. *Frontiers in Pharmacology,* 2025;*15*. https://doi.org/10.3389/fphar.2024.1469887

13. Alhujaily, M., Albukhaty, S., Yusuf, M., Mohammed, M. K. A., Sulaiman, G. M., Al-Karagoly, H., Alyamani, A. A., Albaqami, J., & AlMalki, F. A. Recent advances in plant-mediated zinc oxide nanoparticles with their significant biomedical properties. *Bioengineering,* 2022;*9*(10):541. https://doi.org/10.3390/bioengineering9100541

14. Alhujaily, M., et al. Recent advances in plant-mediated zinc oxide nanoparticles with their significant biomedical properties. *Bioengineering,* 2022;*9*(10):541. https://doi.org/10.3390/bioengineering9100541

15. Sivasankarapillai, V. S., Krishnamoorthy, N., Eldesoky, G. E., Wabaidur, S. M., Islam, M. A., Dhanusuraman, R., & Ponnusamy, V. K. One-pot green synthesis of ZnO nanoparticles using *Scoparia dulcis* plant extract for antimicrobial and antioxidant activities. *Applied Nanoscience,* 2022;*12*:2731–2743. https://doi.org/10.1007/s13204-022-02610-7

16. Mohammadi, S., et al. Green fabrication of zinc oxide nanoparticles using *Phlomis* leaf extract: Characterization and in vitro evaluation of

cytotoxicity and antibacterial properties. *International Journal of Nanomedicine*.2021.

17. Sivasankarapillai, V. S., et al. One-pot green synthesis of ZnO nanoparticles using *Scoparia dulcis* plant extract for antimicrobial and antioxidant activities. *Applied Nanoscience,* 2022;*12*:2731–2743.

18. Vera, J., Herrera, W., Hermosilla, E., Díaz, M., Parada, J., Seabra, A. B., Tortella, G., Pesenti, H., Ciudad, G., & Rubilar, O. Antioxidant activity as an indicator of the efficiency of plant extract-mediated synthesis of zinc oxide nanoparticles. *Antioxidants,* 2023;*12*(4):784. https://doi.org/10.3390/antiox12040784

19. Vera, J., et al. Antioxidant activity as an indicator of the efficiency of plant extract-mediated synthesis of zinc oxide nanoparticles. *Antioxidants,* 2023;*12*(4):784.

20. Pouresmaeil, V., Haghighi, S., Raeisalsadati, A. S., Neamati, A., & Homayouni-Tabrizi, M. The anti-breast cancer effects of green-synthesized zinc oxide nanoparticles using carob extracts. *Anti-Cancer Agents in Medicinal Chemistry,* 2021;*21*(3):316–326. https://doi.org/10.2174/1871520620666200721132522

21. Mongy, Y., & Shalaby, T. Green synthesis of zinc oxide nanoparticles using *Rhus coriaria* extract and their anticancer activity against triple-negative breast cancer cells. *Scientific Reports,* 2024;*14*:13470. https://doi.org/10.1038/s41598-024-63258-7